ESD-TR-91-112

Technical Report
932

Relationships Between Average Radar Power and Steady-State Track Accuracy

W.H. Gilson

27 November 1991

Lincoln Laboratory
MASSACHUSETTS INSTITUTE OF TECHNOLOGY
LEXINGTON, MASSACHUSETTS

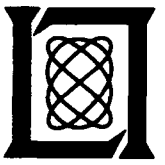

Prepared for the Department of the Navy
under Air Force Contract F19628-90-C-0002.

This report is based on studies performed at Lincoln Laboratory, a center for research operated by Massachusetts Institute of Technology. The work was sponsored by the Department of the Navy under Air Force Contract F19628-90-C-0002.

The ESD Public Affairs Office has reviewed this report, and it is releasable to the National Technical Information Service, where it will be available to the general public, including foreign nationals.

This technical report has been reviewed and is approved for publication.

FOR THE COMMANDER

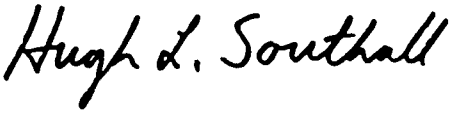

Hugh L. Southall, Lt. Col., USAF
Chief, ESD Lincoln Laboratory Project Office

MASSACHUSETTS INSTITUTE OF TECHNOLOGY
LINCOLN LABORATORY

RELATIONSHIPS BETWEEN AVERAGE RADAR POWER AND STEADY-STATE TRACK ACCURACY

W.H. GILSON
Group 36

TECHNICAL REPORT 932

27 NOVEMBER 1991

LEXINGTON MASSACHUSETTS

ABSTRACT

This report describes a methodology used for relating resources consumed by tracking a maneuvering target to the track accuracy achieved. The methodology accounts for beam shape loss, missed detections, and, in the case of a fire-control radar, reacquisition of the target when it has moved outside the beam. This report presents normalized computational results for the minimum radar power required as a function of the track accuracy, along with the optimal revisit frequencies and the signal-to-noise ratios.

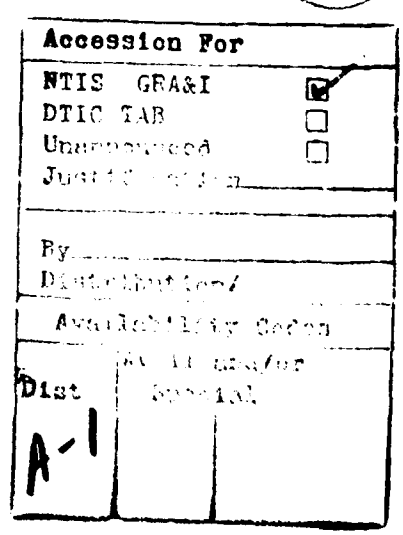

ACKNOWLEDGMENTS

The author is glad to acknowledge his debts to C. B. Chang, M. Gruber, and C. E. Muehe for technical inspiration and encouragement. The computer calculations were carried out by S. McLellan.

TABLE OF CONTENTS

LIST OF ILLUSTRATIONS

LIST OF TABLES

1. INTRODUCTION

This report describes a number of relationships between steady-state target track accuracy and radar power. The work was performed to provide an understanding of the consequences for radar design of the choices of target maneuver and tracking filter models. While the emphasis is on radar power, the methodology and certain results presented here may also be useful in assessing loading on a radar for which time, not average power, is the limited resource.

The accuracy of the track of a given target depends in general on the interval between target measurements and on the accuracy of those measurements; the radar power depends on the update rate, on the signal-to-noise ratio (SNR), and on the number of search beams expended in finding the target for each update. Other authors have addressed the issues of target track accuracy and update rate [1-10] assuming various target and measurement models, but to this author's knowledge, only Muehe and Johnson and Muehe and Goetz [11,12] consider relationships between radar size and tracking accuracy. This report expands upon the previous work to encompass track-while-scan radars as well as dedicated trackers (which we loosely term fire-control radars), several different target maneuver models, and approximate corrections for beam shape losses and target reacquisition after maneuvers. This report does not account for tracking errors due to false alarms or erroneous data associations. Differences between the two types of radars, track-while-scan and dedicated, or fire-control, depend on the notion that the fire-control radar wastes energy reacquiring the target for each update if its track is loose but obtains an advantage in beam shape loss if the track is tight. As in Muehe and Goetz [12], it is assumed that coherent signal integration only is employed. Only the cross-range (azimuth and elevation) track accuracy is considered because the corresponding measurement errors are generally larger than the range errors and dominate the overall tracking error.

2. TARGET MANEUVER MODELS AND TRACKING FILTERS

Because the effectiveness of a tracking filter is determined by the associated target maneuver model, the two will be discussed together. The net effect of choosing each of four combinations of target maneuver models and tracking filters will be summarized in the form of relationships between the track accuracy and the time interval between subsequent measurements. The combinations listed in Table 1 are considered. All random variables in the models are assumed to be zero-mean Gaussian. The equations for Case 1, zero process noise, are given in Miller and Chang [5]; the equations for Cases 2 and 3, step and impulse acceleration, are derived in Pauly [9]; and the equations for correlated random maneuvers, Case 4, are given in Singer [1] with some closed form approximations in Pauly [9] and an exact solution in Beuzit [13]. The constant velocity least squares tracker is considered as a potential worst case that would lead to a rather conservative radar design. The simplest two models, the step and impulse acceleration models, are in Pauly [9], with an additional presentation of the step acceleration model in Friedland [3]. Estrand [10] employs a model of the target's motion wherein the target undergoes an acceleration equivalent to that of white noise passed through a filter whose bandwidth is the inverse of the update time and which is therefore similar to the step acceleration model. The step and impulse models and the model in Estrand [10] can be criticized because they embody the assumption that the target is responsive to the tracker update time, an assumption that may not be accurate. The argument for using these models is that they may represent maneuvers undertaken by a target seeking to evade a tracker; however, step accelerations do not always represent the worst case for the tracker and, furthermore, if the track rate were to exceed the control bandwidth of the target, the model would be unphysical. The Singer model (Case 4) is representative of the attempts to model target maneuvers accurately and to reflect those models in the tracking filters.

For the reader's convenience, the equations used in this study will follow in a uniform notation. We first define some symbols:

T	Track update interval
σ_m^2	Cross-range position measurement variance
σ_x^2	Cross-range position track variance immediately prior to measurement
σ_a^2	Target acceleration variance
τ	Correlation time for target accelerations
K	Number of samples used in linear tracking filter

2.1 Constant Acceleration Target, Constant Velocity Least Squares Tracking Filter

The track variance of a constant velocity tracking filter for a target with constant zero-mean random acceleration is the sum of the variance due to measurement errors and the variance due to the mismatch between the trajectory of the accelerating target and the constant velocity filter.

TABLE 1

Target and Tracker Cases

Case	Target	Filter
1	Constant but random acceleration with zero process noise	Constant velocity least squares fit with optimal data record length
2	Step acceleration — target accelerates randomly after each measurement	Kalman
3	Impulse acceleration — target's velocity changes randomly and instantaneously just prior to each measurement	Kalman
4	Constant acceleration target with correlated white noise maneuvers (Singer model)	Kalman

The track variance due to measurement error alone, just before a new measurement is taken, is given by Chang [8, (2.11)] as

$$2\sigma_m^2 \frac{2K+1}{K(K-1)} \tag{1}$$

and due to the mismatch [8, (2.10)] as

$$\frac{\sigma_a^2 T^4}{4}\left[\frac{(K+1)(K+2)}{6}\right]^2. \tag{2}$$

The complete track variance is

$$\sigma_x^2 = 2\sigma_m^2 \frac{2K+1}{K(K-1)} + \frac{\sigma_a^2 T^4}{144}(K+1)^2(K+2)^2. \tag{3}$$

It will be more convenient to turn this expression around to obtain

$$T = \left(\frac{12\sigma_x}{\sigma_a}\right)^{1/2}\left[\frac{1-2\frac{\sigma_m^2}{\sigma_x^2}\frac{2K+1}{K(K-1)}}{(K+1)^2(K+2)^2}\right]^{1/4}. \tag{4}$$

For a given measurement variance and update time, the tracker employs the optimal number K of data points, the value that minimizes the track variance σ_x^2, or, equivalently, for a given measurement variance and track variance, the value that maximizes the update time T.

2.2 Step and Impulse Acceleration Models, Kalman Tracking Filter

For the step acceleration model, it can be shown that the update time is

$$T = \left[\frac{2\sigma_m}{\sigma_a} \left(\sqrt{1 + \frac{\sigma_x^2}{\sigma_m^2}} + \frac{1}{\sqrt{1 + \frac{\sigma_x^2}{\sigma_m^2}}} - 2 \right) \right]^{1/2}, \tag{5}$$

while for the impulse model the expression for the update time takes the form

$$T = \left[\frac{\sigma_x^4}{\sigma_a \sigma_m^3 \left(2 + \frac{\sigma_x^2}{\sigma_m^2}\right) \sqrt{1 + \frac{\sigma_x^2}{\sigma_m^2}}} \right]^{1/2}. \tag{6}$$

These expressions are obtained by solving the steady-state equations for the elements of the Kalman covariance matrix [9].

2.3 Filtered White Noise Acceleration Model, Kalman Tracking Filter

The situation with a general filtered white noise acceleration process is more difficult. Here Singer is followed [1] and the target acceleration is considered to be a white noise process which is passed through a single pole filter with a pole at $1/\tau$ such that the resulting accelerations have a variance σ_a^2 and a correlation time τ. The power-spectral density of the hypothetical white noise source is $2\sigma_a^2/\tau$. A closed form approximation can be derived [9] for the update time for short correlation times $\tau << t$:

$$T \approx \left[\frac{\sigma_m}{2\eta\sigma_a\sqrt{q_{22}}} \left(\sqrt{1 + \frac{\sigma_x^2}{\sigma_m^2}} - \sqrt{4 + \frac{\frac{\sigma_x^4}{\sigma_m^4}(1 - 4\eta)}{1 + \frac{\sigma_x^2}{\sigma_m^2}}} \right) \right]^{1/2} \tag{7}$$

where

$$\eta \approx \frac{\frac{1}{6} - \frac{1}{2}\left(\frac{\tau}{T}\right)^2 - \frac{1}{2}\left(\frac{\tau}{T}\right)^3}{1 - \frac{3}{2}\left(\frac{\tau}{T}\right)} \tag{8}$$

and

$$q_{22} \approx 2\frac{\tau}{T} - 3\left(\frac{\tau}{T}\right)^2. \tag{9}$$

Because $\tau/t << 1$, η can be replaced with $1/6$ and q_{22} by $2\tau/t$, and the update time is well approximated by

$$T \approx \left[\frac{3\sigma_m}{\sigma_a\sqrt{\frac{2\tau}{T}}}\left(\sqrt{1+\frac{\sigma_x^2}{\sigma_m^2}} + \frac{1}{\sqrt{1+\frac{\sigma_x^2}{\sigma_m^2}}} - \sqrt{4+\frac{\frac{\sigma_x^4}{3\sigma_m^4}}{1+\frac{\sigma_x^2}{\sigma_m^2}}}\right)\right]^{\frac{1}{2}} \tag{10}$$

when $\tau << t$. For longer correlation times, closed form solutions are not available; one must resort to a direct numerical solution of the Riccati equation for the covariance or to the method proposed in Beuzit [13]. In this study, the solution to the steady-state Riccati equation was found by iteration.

3. RADAR POWER AND TRACK ACCURACY FOR A TRACK-WHILE-SCAN RADAR

For a track-while-scan radar, it is assumed that the radar repeatedly scans a given search volume at a fixed repetition interval T_r in a search pattern that is independent of the target's predicted location. The beam shape loss and azimuth measurement accuracy are calculated under the assumption that the target's location has a probability density that is uniform across the beam. The effect of missed detections is accounted for by the approximation that the update interval is replaced by an effective update interval T given by

$$T = T_r / P_D, \tag{11}$$

where the detection probability P_D depends on the SNR (signal energy to white noise power spectral density ratio) ρ of the echo signal. Under the assumed Swerling I target fluctuation model the detection probability is given by [14, (2.4.2)]

$$P_D = (P_{FA})^{\frac{1}{1+\rho}} . \tag{12}$$

A relatively high false alarm probability of 0.001 is assumed for tracking as there are relatively few cells in which the target could reasonably lie; the effects of the ensuing false alarms on the tracker are ignored.

3.1 Radar Measurement Accuracies

The measurement variance of a track-while-scan system is given by

$$\sigma_m^2 \approx \frac{R^2 \theta_3^2}{2 k_m^2 \rho} \tag{13}$$

for a mechanically scanned search radar [14(8.3.1)] and by

$$\sigma_m^2 \approx \frac{1 + (k_m \theta / \theta_3)^2}{2 k_m^2 \rho} R^2 \theta_3^2 \tag{14}$$

for a monopulse radar [14, (8.4.5) and Figure 8.5.9], where

θ	Actual off-boresight angle of the target
θ_3	3 dB receive beamwidth (azimuth and elevation)
k_m	Constant dependent on the beam shape; typically, $k_m \approx 2$

R Range of the target

Both Equations (13) and (14) hold for measurements mode by bistatic as well as monostatic systems (if the SNR ρ includes all beam shape losses and if θ_3 refers to the beam that is making the measurement). On the average, for a track-while-scan system that directs beams with no reference to predicted target locations, θ is uniformly distributed over a disk that is approximately θ_3 in diameter, within whichever beam the target is detected, so that the approximation is made of replacing θ^2 in Equation (14) by its average:

$$\overline{\theta^2} = \frac{4}{\pi\theta_3^2}\int_0^{2\pi}\int_0^{\theta_3/2}\theta^2\,\theta\,d\theta\,d\phi \tag{15}$$

$$= \frac{\theta_3^2}{8}. \tag{16}$$

This replacement yields, for a track-while-scan radar with monopulse angle measurement,

$$\sigma_m^2 \approx \frac{1+k_m^2/8}{2k_m^2\rho}R^2\theta_3^2, \tag{17}$$

or, for the nominal value of $k_m = 2$

$$\sigma_m^2 \approx \frac{R^2\theta_3^2}{5\rho}. \tag{18}$$

In general, the angle measurement variance is the form

$$\sigma_m^2 = \frac{R^2\theta_3^2}{2k_m^2\rho}, \tag{19}$$

where k_m is equal to about 2 for either mechanically scanned or monopulse angle measurement in either a monostatic or a bistatic configuration.

3.2 Radar Power Relationships

For a single pulse, the power needed of a bistatic radar (monostatic is a special case) is given following Nathanson [15, p.57, (2-18)], but with the substitution $G = 4\pi A/\lambda^2$, by

$$P_t = \frac{4\pi\lambda^2 R_1^2 R_2^2 \rho k T_o F_t F_r L}{A_1 A_2 \sigma \tau_c}, \tag{20}$$

where all losses are included in L. For a track-while-scan system, the pattern propagation factors are averaged to produce an overall beam shape loss [16, p.2.4.7]

$$L_B \approx 4 \text{ dB}, \tag{21}$$

included in L. The loss is rounded up because an electronically scanned radar may suffer a loss greater than that of a mechanical scanner [16, p.2.4.7].

If the radar revisits the target every time of interval duration T_r, the power expended on obtaining returns from the target is the energy per visit $P_t \tau_c$ divided by the revisit time,

$$P_{\text{track}} = \frac{P_t \tau_c}{T_r}. \tag{22}$$

The effective track update interval T is, as discussed at the opening of this section, longer than the revisit time by the ratio $1/P_D$. Following Muehe and Goetz [12], the parameters

$$t = T_r \sqrt{\frac{\sigma_a}{R_2 \theta_3}} \tag{23}$$

and

$$\tau_n = \tau \sqrt{\frac{\sigma_a}{R_2 \theta_3}} \tag{24}$$

are defined, where θ_3 is the 3-dB beamwidth,

$$\theta_3 \approx \lambda / \sqrt{A}, \tag{25}$$

corresponding to the measuring aperture. This normalizes all times by a quantity that can be loosely interpreted as the time required for the target to accelerate out of the beam. A normalized track error, the ratio α of the standard deviation of the track error to the beamwidth, is used:

$$\alpha = \sigma_x / R\theta_3. \tag{26}$$

In terms of the normalized update interval, the average power expended on tracking is given by

$$P_{\text{track}} = \frac{4\pi\lambda^2 R_1^2 R_2^2 k T_0 F_t F_r L_R}{A_1 A_2 \sigma} \sqrt{\frac{\sigma_a}{R_2 \theta_3}} \times \frac{L_B \rho}{t}. \tag{27}$$

The normalized track power is the quantity

$$x = L_B \rho / t, \tag{28}$$

the beam pattern loss [excluded from L_R in Equation (27)] times the SNR times the normalized beam rate.

3.3 Computational Results

The track error is obtained by applying the measurement variance and the effective update time relationships described in Section 3.2 to the tracking filter relationships outlined in Section 2. Consider first the dependence of the track power on the SNR and on the track error. Figures 1 through 6 show [as a function of the normalized track error α, defined in Equation (26) and of the per pulse SNR ρ] contours of constant normalized tracking power x for the target and tracker models listed in Table 2. The beam shape loss L_B is included in the normalized tracking power, Equation (28), so that it can be compared to the fire control radar for which the beam shape loss varies with track accuracy. These figures were obtained by calculating the measurement error as a fraction of the beamwidth for each value of the SNR (ordinate) and then applying the relationships of Section 2 to obtain the required track update time to achieve each normalized track error. The normalized power consumption was corrected for the detection probability via Equation (11) and then plotted as contours. For example, in order to achieve a track error of 10 percent of the beamwidth on a target that fits the step acceleration model, Figure 2 shows that with a SNR of 10 dB the normalized power x would be about 25 dB while with a SNR of 25 dB the power requirement would increase by about 5 dB. All of the models shown here display similar behaviors. As expected, the power requirement increases rapidly with decreasing track error, especially for track errors below 20 percent of the beamwidth. The shapes of the contours show that the power required to track a target depends on the available SNR. For low SNRs, less than about 10 dB, the power requirement increases as the probability of detecting the target drops. With very high SNRs, the track accuracy is limited not by the radar's measurement accuracy but rather by the target's maneuvers, and the power requirement increases again. When the two error sources are in balance, the probability of detection is high enough to ensure that few gaps occur in the track, but the measurements are not so accurate that the target's maneuvers dominate the track errors.

The nature of the dependence of the power on the SNR varies with the track error. For low accuracy tracking, the minimum power SNR for a given accuracy is fairly well-defined, varying from about 10 to 12 dB at accuracies of a few beamwidths to about 15 to 20 dB at accuracies of a few tenths of a beamwidth. When very precise tracks are required, better than about a tenth of a beamwidth, the track power is constant over a wide range of SNRs starting from about 10 dB. The lines $P_D = 0.5$ [i.e., $\rho = 13.5$ dB (9.5 dB + L_B)] and $\alpha = \sigma_m/(R_2\theta_3)$, along which the measurement error is equal to the track error, are drawn on each contour plot. To the left of their intersection, the power is largely constant over the range of SNRs that lies between these two lines. To the right of the line $\alpha = \sigma_m/(R_2\theta_3)$, the contours appear to follow straight lines whose slopes reflect

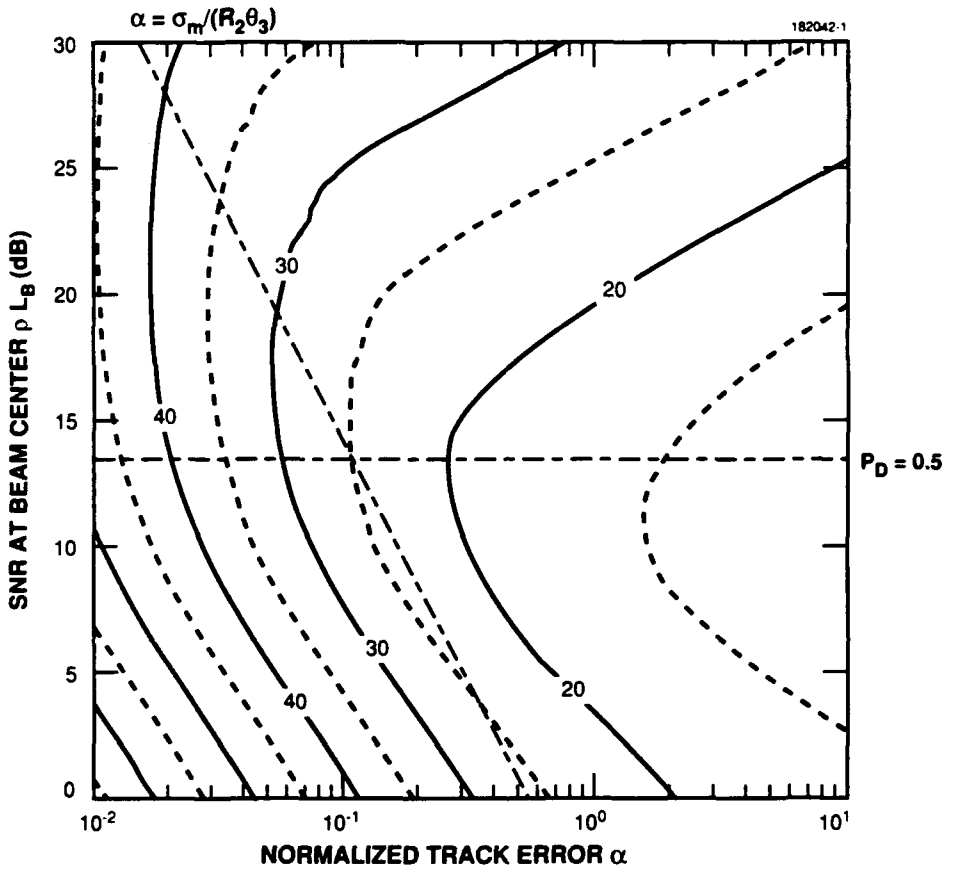

Figure 1. Contours of normalized track-while-scan tracking power x for Case 1, constant acceleration.

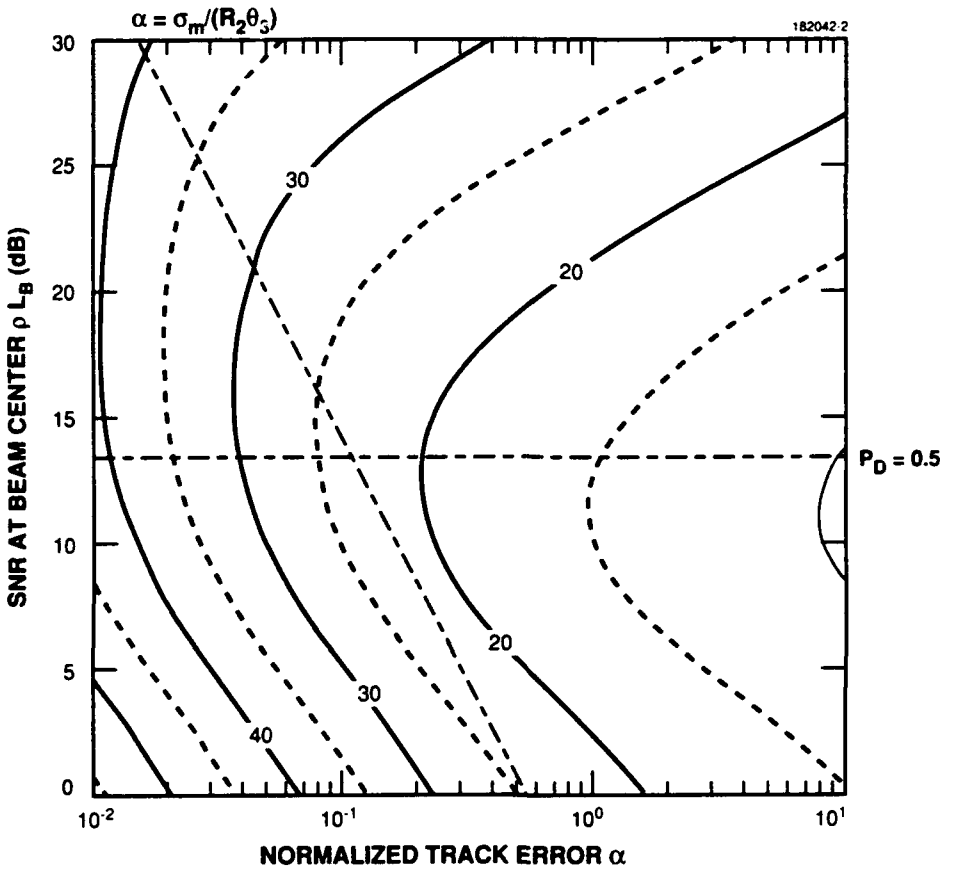

Figure 2. Contours of normalized track-while-scan tracking power x for Case 2, step acceleration.

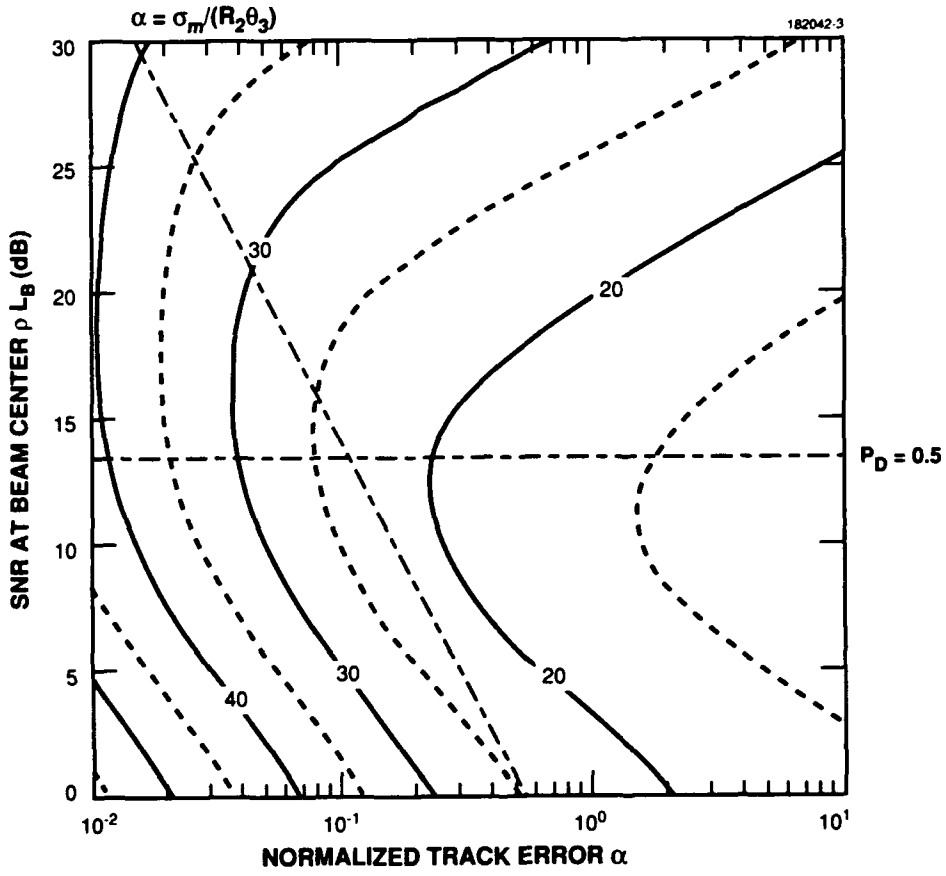

Figure 3. Contours of normalized track-while-scan tracking power x for Case 3, impulse acceleration.

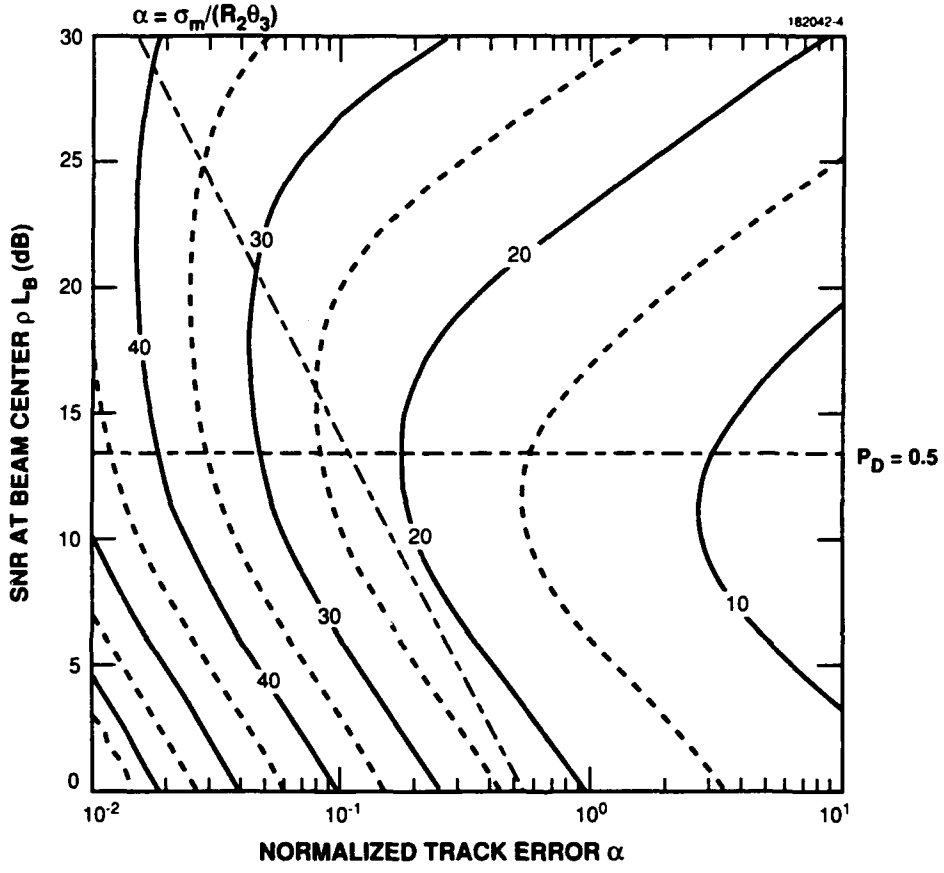

Figure 4. Contours of normalized track-while-scan tracking power x for Case 4a, Singer model, normalized time constant of 0.1.

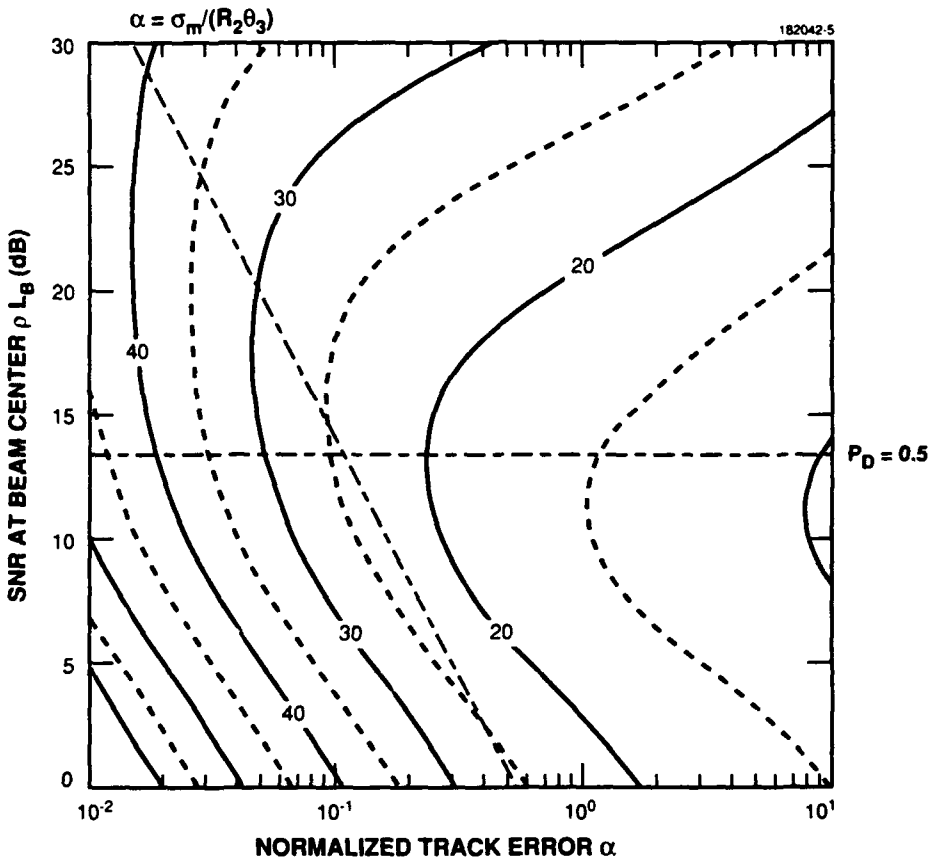

Figure 5. Contours of normalized track-while-scan tracking power x for Case 4b, Singer model, normalized time constant of 1.

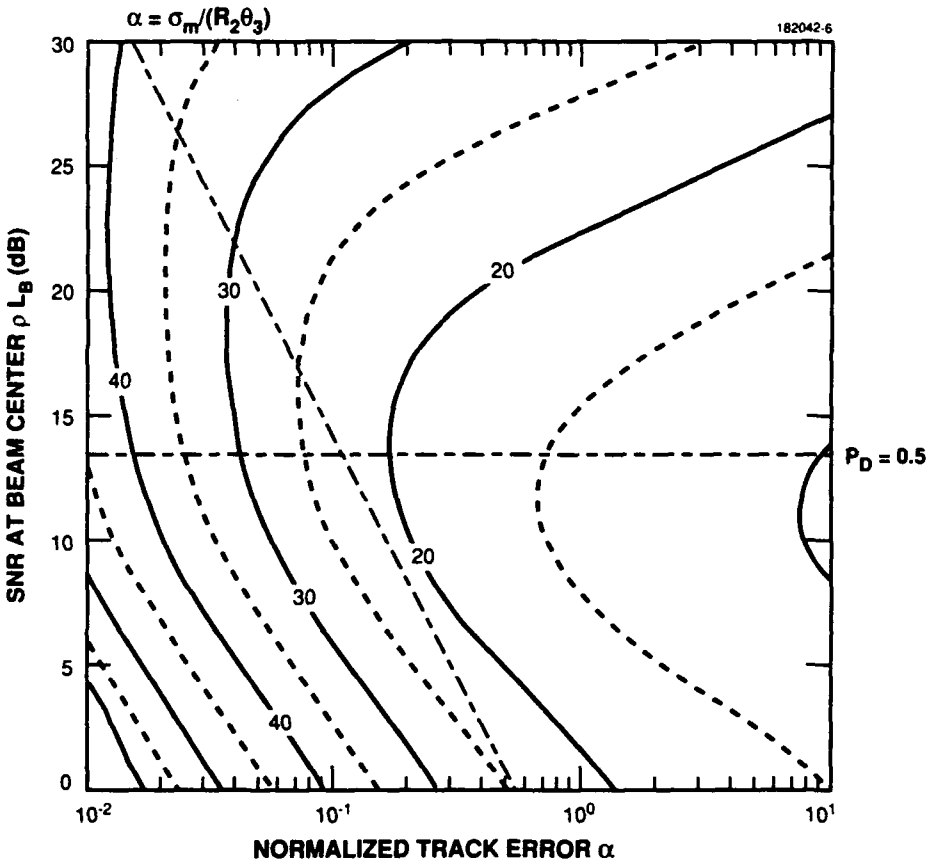

Figure 6. Contours of normalized track-while-scan tracking power x for Case 4c, Singer model, normalized time constant of 10.

TABLE 2

Key to Track-While-Scan Plots

Case	Target	Tracker	Figure
1	Constant acceleration	Constant velocity least squares	1
2	Step acceleration	Kalman filter	2
3	Impulse acceleration	Kalman filter	3
4a	Filtered white noise acceleration, normalized time constant 0.1	Kalman filter	4
4b	Filtered white noise acceleration, normalized time constant 1	Kalman filter	5
4c	Filtered white noise acceleration, normalized time constant 10	Kalman filter	6

the different target maneuver models. For example, with a constant acceleration target the 20-dB normalized power contour has a slope of about 5 dB of SNR per decade of normalized track error above a SNR of about 15 dB. This slope is explained as follows. Along the 20-dB contour, the ratio of the SNR to the normalized update time is constant and equal to 100. Because the SNRs are above the $\alpha = \sigma_m/(R_2\theta_3)$ line, the measurement accuracy exceeds the track accuracy and the track accuracy is limited by the target's acceleration. For the constant acceleration target considered here, the normalized track error in this regime is given roughly by $\alpha \approx \sigma_a T^2/(2R_2\theta_3)$, where σ_a is the standard deviation of the target's acceleration and T is the update time. Because the normalized update time is proportional to the real update time T [Equations (11) and (23)], for constant power the SNR varies as t, which in turn varies as $\alpha^{1/2}$. Thus one should indeed expect to find that for large SNRs the curves of constant power are straight lines at 5 dB per decade. For high SNRs, the step and impulse acceleration models are similar to the constant acceleration model in the respect that the track error depends on the square of the update time. Under the filtered white noise model the track error depends on the square of the update time when the correlation item is longer than the update time, but when the correlation time is shorter than the update time the target's velocity executes a "drunkard's walk" between updates and the track error depends on the 3/2 power of the update time. This agrees with the 7.5 dB per decade slope of the normalized power contours for large SNRs in Figure 4. Figure 6, with a normalized time constant of 10, shows behavior similar to but not identical to that of the first three models while Figure 5, at a unity normalized time constant, shows the beginnings of a transition between the two regimes around a normalized track error of 3 beamwidths.

Figure 7(a) shows for each case the "best" that one can achieve, i.e., the minimum normalized power x that can produce the desired track accuracy; Figure 7(b) shows the beam shape loss L_B times the SNR ρ at which that minimum is achieved; and Figure 7(c) shows the corresponding normalized update rate $1/t$. It is immediately apparent that the constant velocity least squares tracker model, Case 1, is the most pessimistic. This is expected because the filter is not an optimal tracking filter. The step and impulse acceleration models, Cases 2 and 3, are the most optimistic, especially where the track errors are small. Under these models, in order to achieve these small track errors, one obtains the smallest power requirement by increasing the update rate above the rate for any of the other cases and by simultaneously dropping the SNR. This operating point is optimal because the step and impulse models assume that the targets maneuver ever more rapidly as the update rate increases. Because the standard deviation of the maneuver acceleration is held constant, when the maneuvers occur more rapidly, the target travels shorter distances as net results of these maneuvers. Hence the optimal strategy for the tracker is skewed towards more rapid updates to reduce the net effect of the target's maneuvers. One can conclude that the step and impulse acceleration targets are easier to track because their maneuvers are slaved to the radar's update rate, and it is consequently doubtful that they are good benchmarks against which to design and evaluate tracking radar sets with small track errors. When the track error is large, the situation is reversed because the update times are relatively long, and under the step and impulse models the target accelerates at a constant rate until the next update. In this large track error region, the step and impulse models are similar to the constant velocity least squares filter, constant acceleration model as the errors are dominated by the constant but unknown acceleration between updates. The Singer target model falls roughly in the middle. When the required track error is small, the long time constant target ($\tau = 10$) is easier to track because the filter can produce an accurate estimate of the acceleration. When the desired track error is relatively large, the short time constant target ($\tau = 0.1$) requires less power to track, because over the relatively long interval between updates the target maneuvers many times and produces a smaller net displacement. Although the Singer model may be more realistic if the tracking filter is indeed matched to the characteristics of the target, it can be argued that one should base the design of a tracker on a more conservative construct such as the constant velocity linear least squares filter, constant acceleration target model.

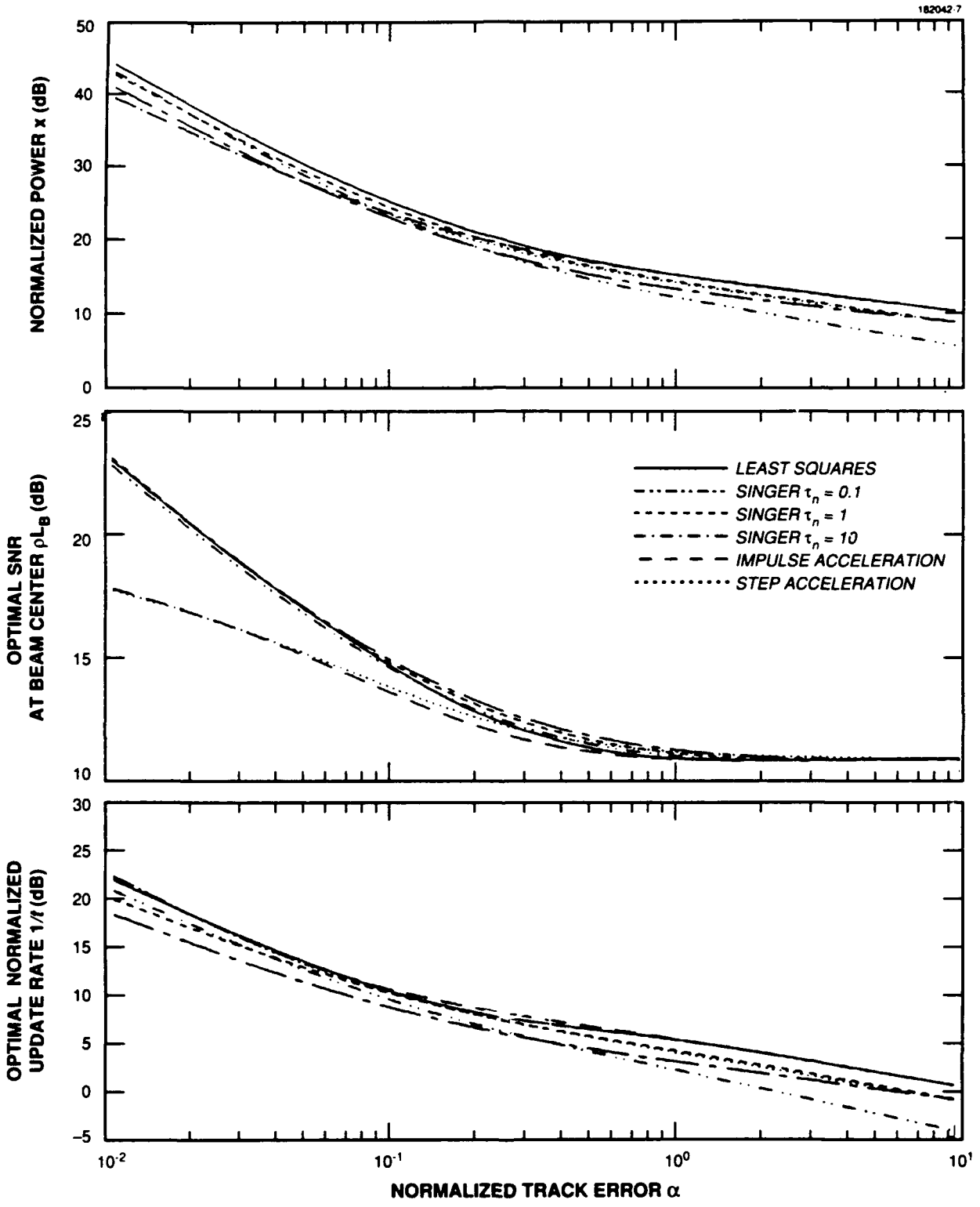

Figure 7. Optimal track-while-scan operating points.

4. RADAR POWER AND TRACK ACCURACY FOR A DEDICATED TRACKER

When tracking a target using a dedicated radar instead of tracking while scanning, two changes occur. First, the target's location within the beam is not always uniformly distributed across the beam but is, for the tighter tracks, distributed as a Gaussian random variable with its maximal probability density near the center of the beam. Second, there is always a nonzero probability that the first tracking dwell in each update will miss the target because the target has maneuvered outside the beam. These two changes introduce factors into the normalized tracking power that penalize the radar for keeping too loose a track of the target. A track accuracy will appear that is optimal in the sense that it requires the least radar power to maintain a track of the object.

4.1 Target Acquisition Loss

With a relatively loose target track, the radar will at times have to search more than one beamwidth for the target in order to update the track. The number of beams searched is given approximately by

$$\tilde{n}(\psi, \phi) \approx \max \left[1,\, 4\left(\psi^2 + \phi^2\right) / \theta_3^2\right], \tag{29}$$

where ψ and ϕ locate the target in azimuth and elevation relative to its predicted location and where θ_3 is the 3-dB beamwidth. This expression is based on the assumption that the search volume of the tracker exactly matches the required search volume, an assumption that is probably optimistic as the radar's search volume is likely to be "quantized" in units at least as large as the solid angle of the radar beam. The expected value n of the number of search beams is written in terms of the probability density of the target angles, assuming that ψ and ϕ are both $N(0, \sigma_\psi^2)$,

$$p(\psi, \phi) = \frac{1}{2\pi\sigma_\psi^2} \exp\left[-\frac{\psi^2 + \phi^2}{2\sigma_\psi^2}\right], \tag{30}$$

as

$$n = \mathrm{E}\,\tilde{n} \tag{31}$$

$$= \int_{-\infty}^{\infty} d\psi \int_{-\infty}^{\infty} d\phi\, \tilde{n}(\psi, \phi)\, p(\psi, \phi). \tag{32}$$

Letting $\gamma = (\psi^2 + \phi^2)^{1/2}$ and $\beta = \tan^{-1} \psi/\phi$, performing the indicated change of variables, and integrating over β, one finds that the expected value can be written as

$$n = \frac{1}{\sigma_\psi^2} \int_0^\infty \gamma \, d\gamma \max\left(1,\, 4\gamma^2/\theta_3^2\right) \exp[-\gamma^2/2\sigma_\psi^2]. \tag{33}$$

The integral is performed in two stages, one from zero to $\theta_3/(2\gamma)$ and the other from $\theta_3/(2\gamma)$ to ∞. Upon identifying σ_ψ as $\alpha\theta_3$, one finds that the expected number of beams to search is

$$n = 1 + 8\alpha^2 \exp\left[-1/8\alpha^2\right]. \tag{34}$$

This factor multiplies the tracking power directly. The missed detections, when the target is indeed within the beam but not detected, constitute a further drain on the radar's power. The number of times on the average that a radar with detection probability P_D will have to scan a given search volume in order to find a target known to be in that search volume is

$$m = 1 + (1 - P_D) + (1 - P_D)^2 + (1 - P_D)^3 + \cdots \tag{35}$$

$$= 1/P_D. \tag{36}$$

This factor too multiplies the required radar power.

4.2 Beam Shape Loss

Section 3 assumed that the average beam shape loss was fixed. With a dedicated tracker, the expected distance of the target from the center of the beam in which it is detected depends on the track accuracy. A simple calculation can be performed for the loss associated with the off-bore sight displacement under the assumption that the beam shape is Gaussian. The magnitude of the round-trip pattern propagation factor is

$$|H(\psi, \phi)|^2 = \exp\left[-(4 \ln 2)\left(\psi^2 + \phi^2\right)/\theta_3^2\right]. \tag{37}$$

Assuming that the radar antenna is directed at the expected location of the target and that the target tracking errors are Gaussian and symmetrical about the bore sight, the density function of the target's location relative to the boresight is given by Equation (30). The expected round-trip beam shape gain due to the target's deviation from the center of the beam is

$$G_b = \int_{-\infty}^{\infty} d\psi \int_{-\infty}^{\infty} d\phi \; |H(\psi, \phi)|^4 \, p(\psi, \phi). \tag{38}$$

The integrals are separable and equal, and so the loss can be written as

$$G_b = \frac{1}{2\pi\sigma_\psi^2}\left(\int_{-\infty}^{\infty} d\psi \exp\left[-\psi^2\left(\frac{8\ln 2}{\theta_3^2}+\frac{1}{2\sigma_\psi^2}\right)\right]\right)^2, \tag{39}$$

which evaluates to

$$G_b = \frac{1}{16\alpha^2 \ln 2 + 1}. \tag{40}$$

Equivalently, the beam shape loss is

$$L_b = 16\alpha^2 \ln 2 + 1. \tag{41}$$

Implicit in this expression is the assumption that the beam shape loss increases indefinitely with increasing track variance, whereas in fact once the track is loose enough for multiple beams to be required for reacquisition, the beam shape loss reaches the track-while-scan asymptote of about 4 dB [16, p.2.47]. The effective beam shape gain is approximated as the gain under the assumption that the target lies within the first beam weighted by the probability that the target does indeed lie within that beam, summed with the asymptotic search gain of −4 dB weighted by the probability that the target lies outside the first beam:

$$G_B = \frac{1}{16\alpha^2 \ln 2 + 1}\left[1 - \exp\left(-\frac{1}{8\alpha^2}\right)\right] + 10^{-0.4}\exp\left(-\frac{1}{8\alpha^2}\right). \tag{42}$$

The average beam shape loss is the inverse of the beam shape gain.

4.3 Measurement Accuracy

Equation (13) gives the measurement variance for a monopulse radar as a function of the angle θ between the target and the center of the beam. The expected value of the variance over the distribution of the off-axis angle is obtained by replacing θ^2 in Equation (13) by its expected value $2\sigma_\psi^2$. The expression

$$\sigma_m^2 \approx \frac{1 + 2k_m^2\alpha^2}{2k_m^2\rho} R^2\theta_3^2 \tag{43}$$

is used for the effective measurement variance as a function of the normalized track accuracy. As the track variance may exceed one beamwidth, the logic that led to Equation (42) here leads to

$$\sigma_m^2 \approx \frac{[1+2k_m^2\alpha^2]\left[1-\exp\left(-\frac{1}{8\alpha^2}\right)\right]+[1+k_m^2/8]\exp\left(-\frac{1}{8\alpha^2}\right)}{2k_m^2\rho} R^2\theta_3^2. \tag{44}$$

4.4 Radar Power Computations

The radar power requirement still obeys Equation (27), but the interpretation of the loss varies. The loss is written as

$$L = nmL_B L_R \tag{45}$$

where the number n of search beams per dwell is given by Equation (34), the number m of visits to detect the target is given by Equation (36), the effective beam shape loss is obtained by inverting Equation (42), and where L_R incorporates the remaining radar loss factors. Figures 8 through 13 show contours of constant normalized dedicated beam track power,

$$x = \frac{nL_B\rho}{t}. \tag{46}$$

Note that the factor of m is already incorporated in the definition of the normalized time t via Equations (11) and (23).

TABLE 3

Key to Dedicated Tracker Plots

Case	Target	Tracker	Figure
1	Constant acceleration	Constant velocity least squares	8
2	Step acceleration	Kalman filter	9
3	Impulse acceleration	Kalman filter	10
4a	Filtered white noise acceleration, normalized time constant 0.1	Kalman filter	11
4b	Filtered white noise acceleration, normalized time constant 1	Kalman filter	12
4c	Filtered white noise acceleration, normalized time constant 10	Kalman filter	13

The contours for the fire-control radar exhibit substantially the same behaviors as those for the track-while-scan radar, so long as the track accuracy is better than about a tenth of a beamwidth. The power levels for the fire-control radar are about 4 dB lower because the radar tries to maintain the target in the center of the beam, thereby minimizing the beam shape loss. Once the radar allows the track accuracy to deteriorate, the likely number of beams that it will have to search to find the target grows dramatically. With track errors larger than about a beamwidth and SNR values greater than about 10 dB, the curves of constant track power exhibit a proportionality to α^{-2} in place of the positive powers seen with the track-while-scan radar. This dependence reflects the severe penalty imposed on the radar for reacquiring loosely tracked targets. For a fixed power level, the SNR is given by $\rho = xt/(nL_B)$. As t is a relatively weak function of the track accuracy for large α (*cf.* Figures 1 through 6), and as L_B is nearly constant at 4 dB for large α, the contours are controlled largely by the number of search beams n, a number that is proportional to the square of the track error.

Figure 14 was prepared by analogy with Figure 7. Because the power contours in Figures 8 through 13 are bowl-shaped, there is, as Figure 14 discloses, a track accuracy that is optimal in terms of minimizing the tracking power. This accuracy is about a quarter of a beamwidth. The "bump" in the beam-center SNR, ρL_B, is a result of higher beam pattern losses at track accuracies that place the target often near the edge of the beam. These calculations ignore the cost of a track-while-scan radar's surveillance (at the same update rate as the tracked target) away from the target's true location; they should not be construed to imply that tracking with such a radar is "cheaper" than tracking with a fire-control radar. Figure 14 shows that to maintain track of a target with a fire control radar at minimal cost one should choose a dwell rate of $n/t \approx 6$ (normalized) at about an 11-dB SNR. The interval between radar beams on target will be

$$T = t\sqrt{\frac{R\theta_3}{\sigma_a}}, \tag{47}$$

and the number of radar beams to acquire the target per update will be equal to n evaluated at $\alpha \approx 1/4$. At the minimum, via Equation (34), $n \approx 1$. For example, with a 10 mrad beam at 50-km range, about two beams per second will be needed to maintain track of a $5g$ target at a minimum power level. Maintaining a track accuracy of a tenth of a beamwidth with a fire-control radar requires a normalized update rate of about 10 at a SNR of about 11 dB (discarding the impulse and step acceleration results). Continuing with the example, one finds the update rate to be about 3 Hz. The SNR at beam center and the power required to maintain this track accuracy would be about 4 dB higher for a track-while-scan radar (Figure 7). At the much coarser track accuracy of, say, 2 beamwidths, one finds significant differences between the behaviors of track-while-scan and fire-control radars. A track-while-scan radar would require a normalized update rate of 1.6 at a beam center SNR of about 11 dB, while the fire-control radar has to search about 30 beams and requires a normalized dwell rate of about 50. Because of its search, the fire-control radar suffers the same loss of 4 dB as would the track-while-scan radar. Carrying our example forward, the

track-while-scan radar has a 0.5-Hz update rate while the fire-control radar has to generate 13 beams per update for an effective dwell rate of about 6 Hz.

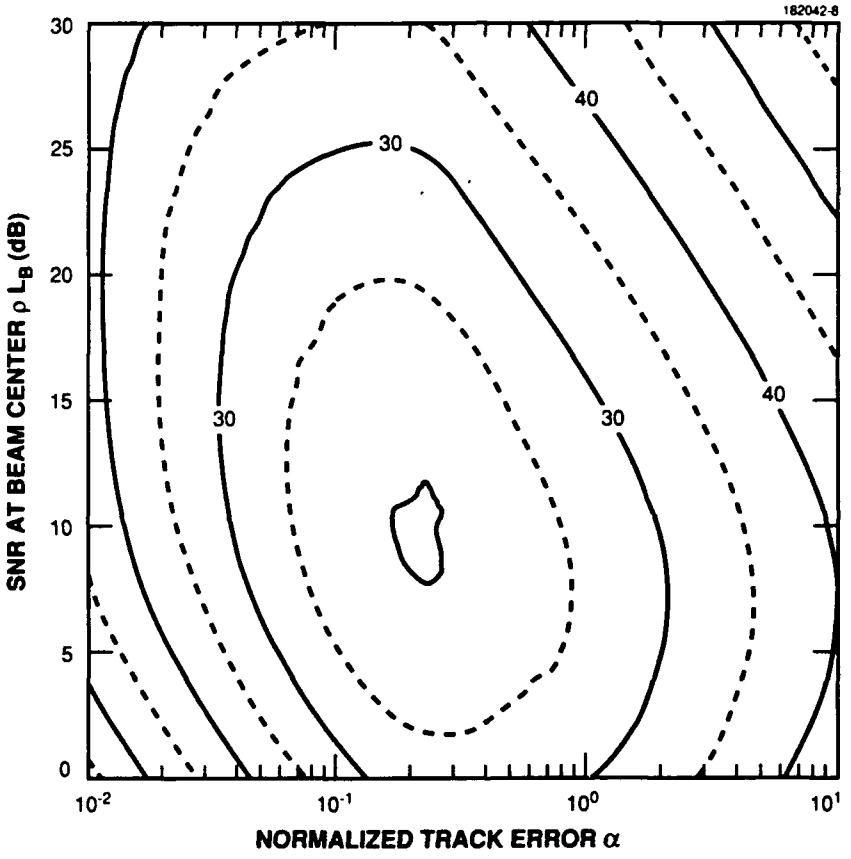

Figure 8. Contours of normalized fire-control tracking power x for Case 1, constant acceleration.

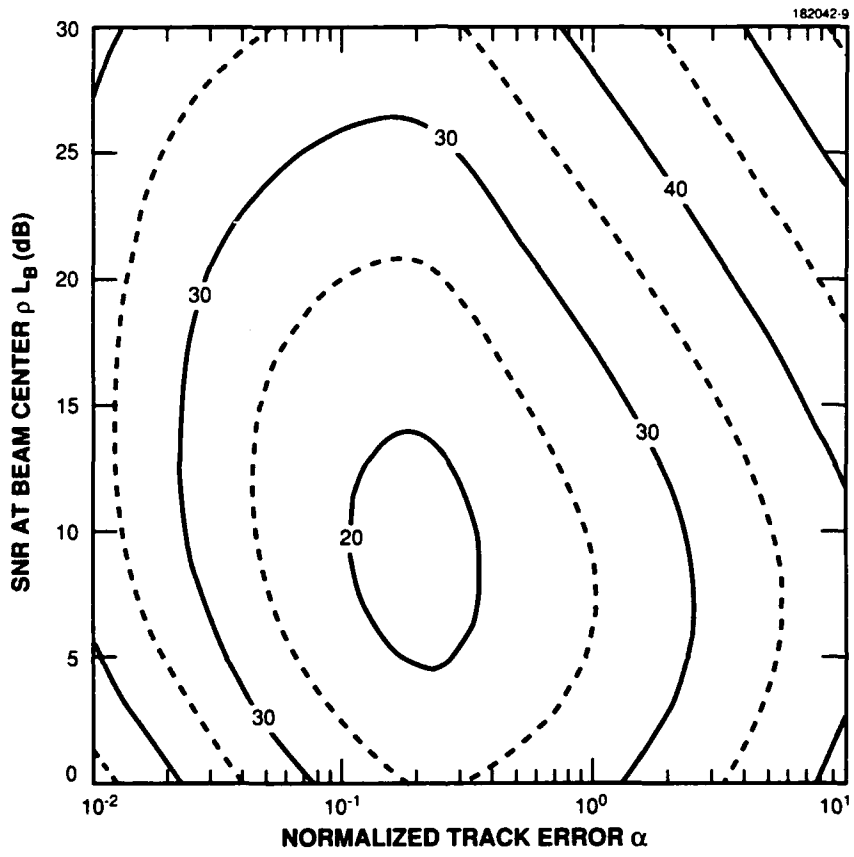

Figure 9. Contours of normalized fire-control tracking power x for Case 2, step acceleration.

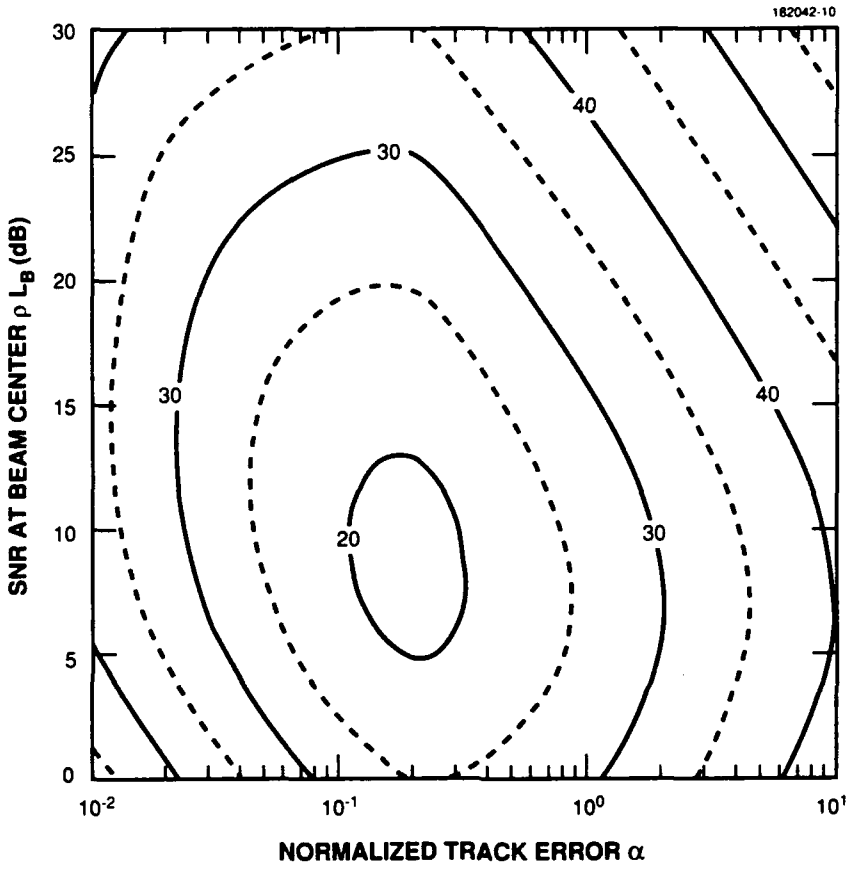

Figure 10. Contours of normalized fire-control tracking power x for Case 3, impulse acceleration.

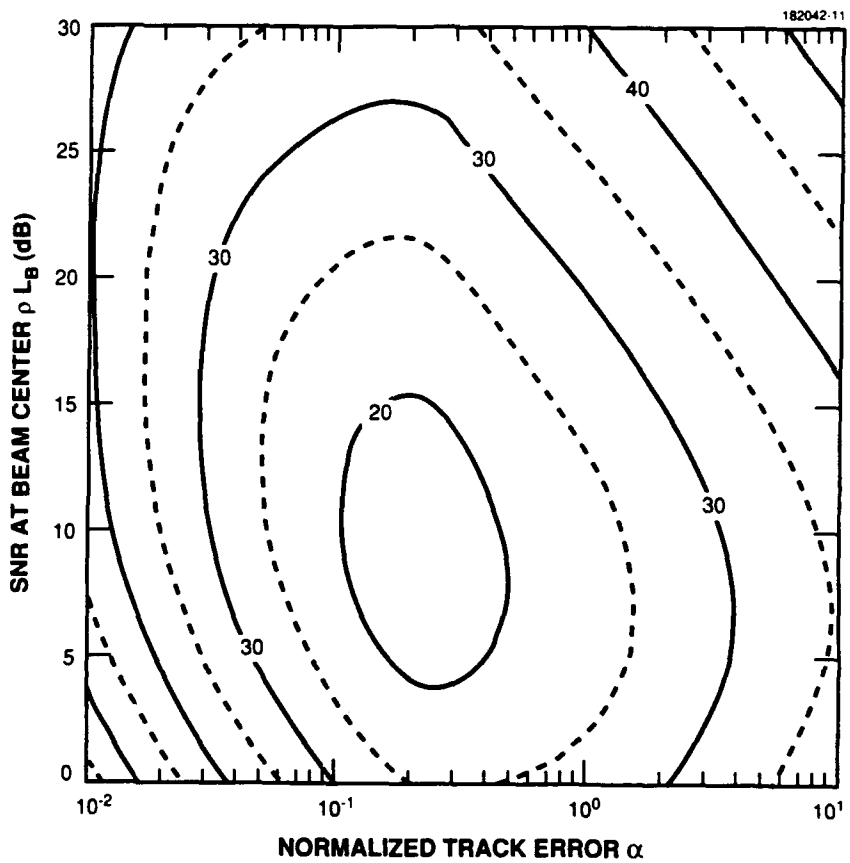

Figure 11. Contours of normalized fire-control tracking power x for Case 4a, Singer model, normalized time constant of 0.1.

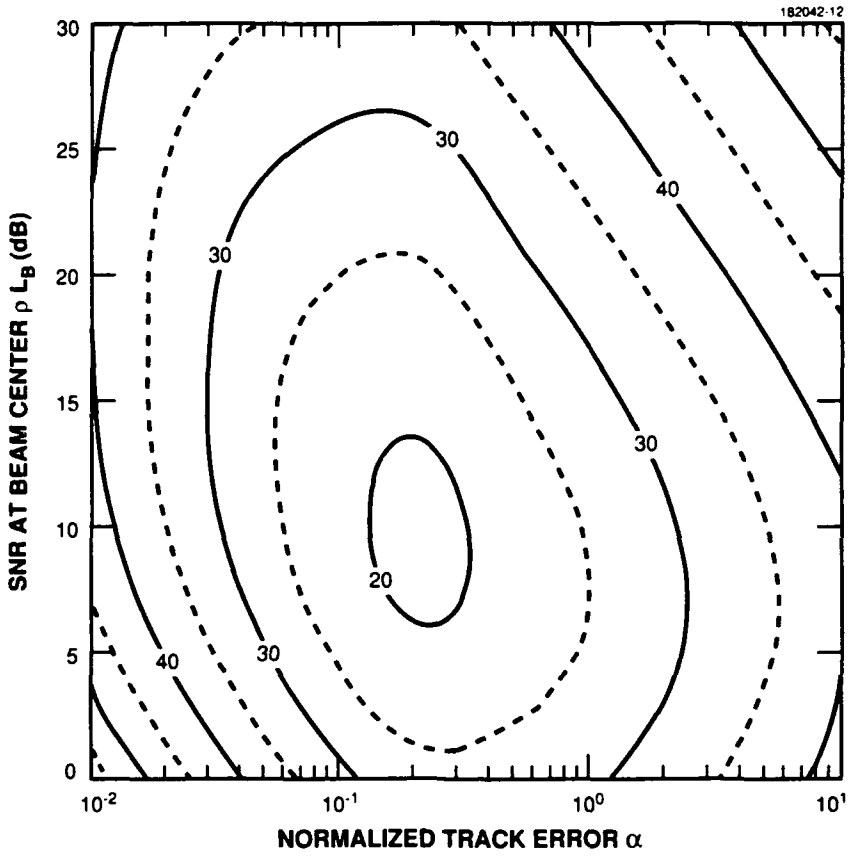

Figure 12. Contours of normalized fire-control tracking power x for Case 4b, Singer model, normalized time constant of 1.

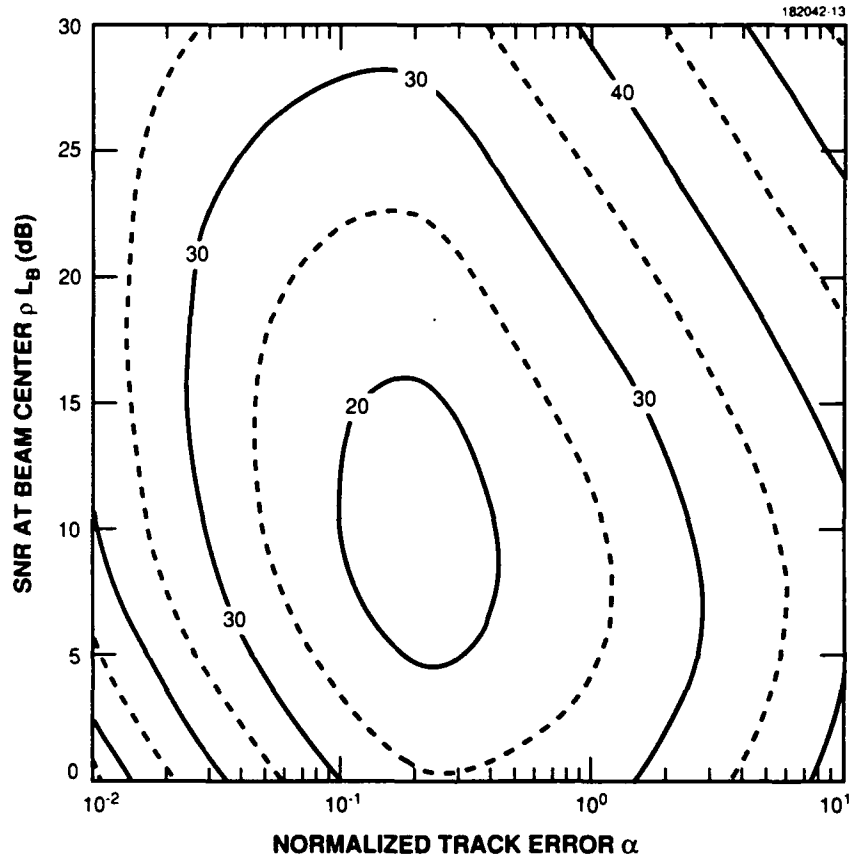

Figure 13. Contours of normalized fire-control tracking power x for Case 4c, Singer model, normalized time constant of 10.

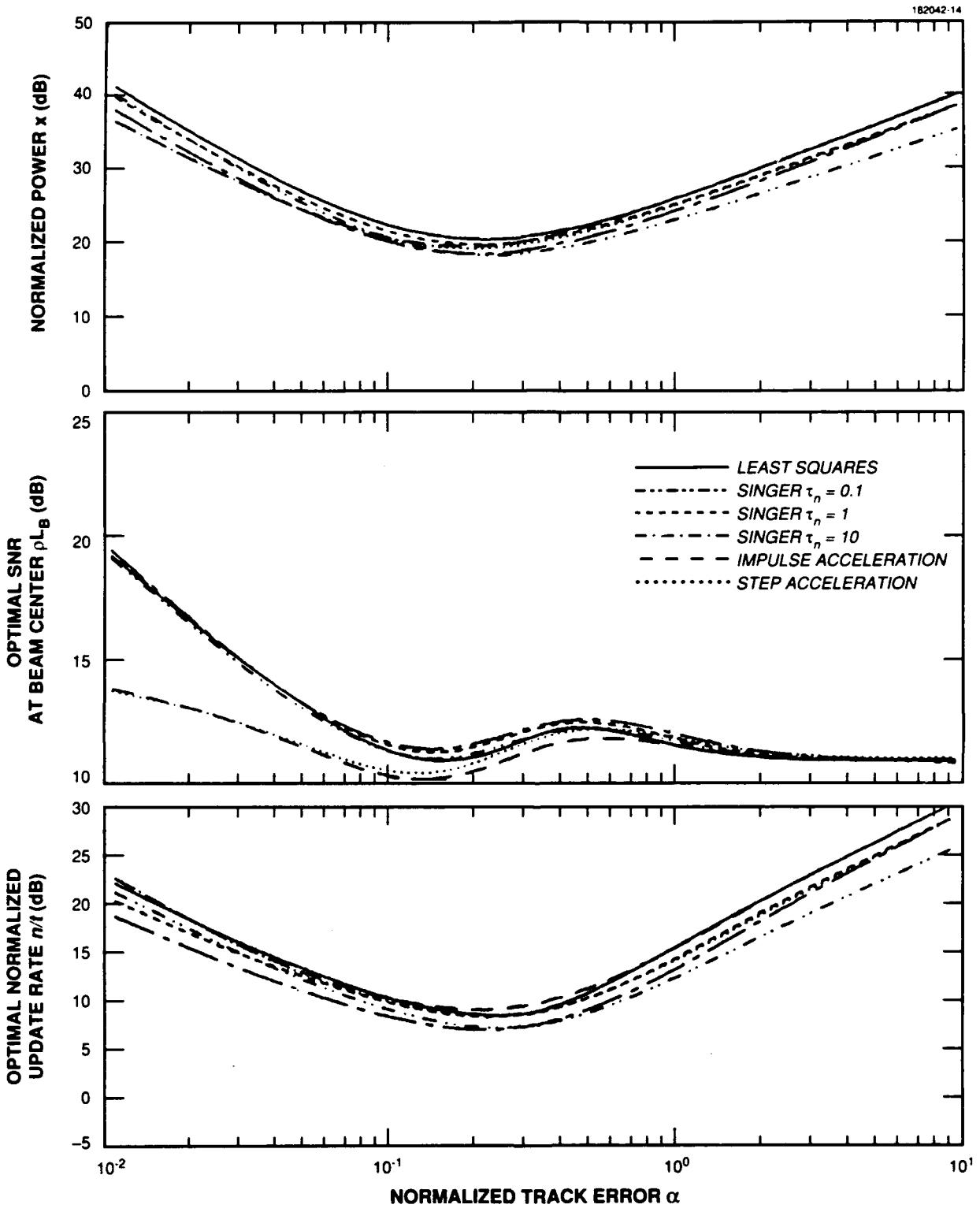

Figure 14. Optimal fire-control operating points.

5. DISCUSSION

Perhaps the most useful conclusion to be drawn from these calculations is that the radar load is relatively insensitive to the details of the target and tracker models. The spread between the models is at most 6 dB in normalized power over a 3 decade range in normalized track accuracies, for both track-while-scan and fire-control radars. If one excludes the somewhat unrealistic step and impulse acceleration models, the spread in power is only 4 dB over a similar range of update rates. All of the models show a minimum in the power needed to maintain track at a track accuracy of about a quarter of a beamwidth for a fire-control radar and a power requirement that decreases monotonically with increasingly coarser tracking for a track-while-scan radar. One is thus not likely to be very wrong no matter which model one chooses. One should, however, be perhaps a bit suspicious of high accuracy track calculations based on such models as the step and impulse models in which the bandwidth of the target's maneuvers is tied to the update rate of the radar.

The track accuracies in this report are "instantaneous" position accuracies just before the measurements are taken and are applicable to tasks that are accomplished within one measurement interval, before the target has time to stray very far. Thus they are applicable to track maintenance or to handing off targets to other sensors. To evaluate the cost of maintaining a track of sufficient quality to vector an interceptor to the target, one would need to evaluate a prediction accuracy.

The calculations shown here were predicated on a Swerling I target; the results would change particularly where the detection probability is less than about 0.5 were a different fluctuation model assumed. There would also be some changes if the radar employed noncoherent integration instead of only coherent integration as assumed here. In either case, it is expected that the overall conclusions regarding the consequences of different target and tracker models and the overall behavior of the power, SNR, and update rate as a function of track accuracy would remain unchanged.

REFERENCES

1. R. A. Singer, "Estimating Optimal Tracking Filter Performance for Manned Maneuvering Targets," *IEEE Trans. Aerosp. Electron. Syst.*, AES-6, pp. 473–483 (July 1970).

2. R. J. Fitzgerald, "Dimensionless Design Data for Three-State Tracking Filters," in *Proc. Joint Automatic Control Conference*, pp. 129–130 (1971).

3. B. Friedland, "Optimum Steady-State Position and Velocity Estimation Using Noisy Sampled Position Data," *IEEE Trans. Aerosp. Electron. Syst.*, AES-9, pp. 906–911 (November 1973).

4. G. van Keuk, "Adaptive Computer Controlled Target Tracking with a Phased Array Radar," in *Proc. IEEE 1975 International Radar Conference*, pp. 429–434 (April 1975).

5. R. W. Miller and C. B. Chang (private communication, 1977).

6. F. R. Castella, "An Adaptive Two-Dimensional Kalman Tracking Filter," *IEEE Trans. Aerosp. Electron. Syst.*, AES-16, pp. 822–829 (November 1980).

7. R. J. Fitzgerald, "Simple Tracking Filters: Steady-State Filtering and Smoothing Performance," *IEEE Trans. Aerosp. Electron. Syst.*, AES-16, pp. 860–864 (November 1980). Errata: 1981, p. 305.

8. C. B. Chang, "A Model for Sensor-Interceptor Trade-Off Analysis," Technical Report 599, Lincoln Laboratory, Massachusetts Institute of Technology, Lexington, Massachusetts (January 1982), DTIC AD-A112046.

9. J. M. Pauly (private communication, 1983).

10. B. Ekstrand, "Analytical Steady State Solution for a Kalman Tracking Filter," *IEEE Trans. Aerosp. Electron. Syst.*, AES-19, pp. 815–819 (November 1983).

11. C. E. Muehe and A. B. Johnson (private communication, 1987).

12. C. E. Muehe and B. Goetz (private communication, 1988).

13. M. Beuzit, "Analytical Steady-State Solution for a Three-State Kalman Filter," *IEEE Trans. Aerosp. Electron. Syst.*, AES-25, pp. 828–835 (November 1989).

14. D. K. Barton, *Modern Radar System Analysis* (Artech House, Dedham, Massachusetts, 1988).

15. F. E. Nathanson, *Radar Design Principles, Signal Processing and the Environment* (McGraw-Hill, New York, 1969).

16. M. I. Skolnik, ed., *Radar Handbook*, second ed. (McGraw-Hill, New York, 1990).

REPORT DOCUMENTATION PAGE

Form Approved
OMB No. 0704-0188

1. AGENCY USE ONLY (*Leave blank*)	2. REPORT DATE	3. REPORT TYPE AND DATES COVERED
	27 November 1991	Technical Report

4. TITLE AND SUBTITLE

Relationships Between Average Radar Power and Steady-State Track Accuracy

5. FUNDING NUMBERS

C — F19628-90-C-0002
PE — 63103N, 62712N
PR — 401

6. AUTHOR(S)

William H. Gilson

7. PERFORMING ORGANIZATION NAME(S) AND ADDRESS(ES)

Lincoln Laboratory, MIT
P.O. Box 73
Lexington, MA 02173-9108

8. PERFORMING ORGANIZATION REPORT NUMBER

TR-932

9. SPONSORING/MONITORING AGENCY NAME(S) AND ADDRESS(ES)

AAW
Department of the Navy
Washington, DC 20350

10. SPONSORING/MONITORING AGENCY REPORT NUMBER

ESD-TR-91-112

11. SUPPLEMENTARY NOTES

None

12a. DISTRIBUTION/AVAILABILITY STATEMENT

Approved for public release; distribution is unlimited.

12b. DISTRIBUTION CODE

13. ABSTRACT (*Maximum 200 words*)

This report describes a methodology used for relating resources consumed by tracking a maneuvering target to the track accuracy achieved. The methodology accounts for beam shape loss, missed detections, and, in the case of a fire-control radar, reacquisition of the target when it has moved outside the beam. This report presents normalized computational results for the minimum radar power required as a function of the track accuracy, along with the optimal revisit frequencies and the signal-to-noise ratios.

14. SUBJECT TERMS

radar, tracking, loading, losses, optimization, target model, tracking filter, update rate, track accuracy, maneuvering target

15. NUMBER OF PAGES
50

16. PRICE CODE

17. SECURITY CLASSIFICATION OF REPORT	18. SECURITY CLASSIFICATION OF THIS PAGE	19. SECURITY CLASSIFICATION OF ABSTRACT	20. LIMITATION OF ABSTRACT
Unclassified	Unclassified	Unclassified	